EVTC

Electric Vehicle Transportation Center

Initial Conditioning Characterization Test and other preliminary testing

Matthieu Dubarry & Arnaud Devie

Hawaii Natural Energy Institute

University of Hawaii at Manoa

1680 East West Road, POST 109

Honolulu, HI 96822

E-mail: matthieu@hawaii.edu

Submitted to:

Dr. David Block

Florida Solar Energy Center
University of Central Florida

1679 Clearlake Road

Cocoa, FL 32922

E-mail: block@fsec.ucf.edu

Purchase Order Number: 291166

Report Number: HNEI-06-15

February 2015

HNEI
Hawai'i Natural Energy Institute
School of Ocean and Earth Science and Technology
University of Hawai'i at Mānoa

Acronyms and Abbreviations

BOD	Beginning of discharge
BSF	Battery sizing factor
EOD	End of discharge
G2V	Grid to vehicle
ICCT	Initial conditioning and characterization test
IQR	Inter quartile range
OCV	Open circuit voltage
RCV	Rest cell voltage
SOC	State of charge
SOH	State of health
V2G	Vehicle to grid

TABLE OF CONTENTS

INITIAL CONDITIONING CHARACTERIZATION TEST AND OTHER PRELIMINARY TESTING

Submitted by:
Hawaii Natural Energy Institute

1 ABSTRACT

This report summarizes results of the first stage of the testing plan implemented by the Hawaii Natural Energy Institute (HNEI) to evaluate Electric Vehicle battery durability and reliability under electric utility grid operations. Commercial EV battery cells are tested in order to assess the impact of vehicle to grid and grid to vehicle applications on cell degradation. In this report the focus is on the description of the initial conditioning and characterization test (ICCT), showcasing the intrinsic cell-to-cell variations. This report also introduces a slight modification to the previously reported test plan and provides a status update on the ongoing testing.

2 INTRODUCTION

In our previous report [1] we proposed a test plan based on the application of design of experiments techniques for both the cycling and the calendar aging study. With this plan, we should be able to assess the impact of vehicle to grid (V2G) and grid to vehicle (G2V) strategies as well as the impact of charging habits on lithium-ion (Li-ion) cells. This report showcases the implementation of the initial conditioning and characterization test (ICCT) phase.

The new state-of-the-art HNEI battery testing laboratory located at HNEI's Hawaii Sustainable Energy Research Facility (HiSERF) in Honolulu has been operational since April 15th 2015, when the initial conditioning and characterization testing was initiated. Within this new laboratory, an Arbin battery tester is used in conjunction with an AMEREX temperature chamber to carry out testing exclusively associated with this project (Figure 1). A total of 40 channels are available, each capable of sourcing or sinking 25A at voltages up to 5V. Unless otherwise specified, ambient temperature is set to 25°C. Prior to the testing, all channels were current and voltage calibrated against a common reference (NIST-traceable Keithley 2700 source meter unit) to ensure consistency across the experiment.

The selected Panasonic NCR18650B cells[1] have a 3200 mAh rated capacity and the manufacturer specification sheet is available in appendix 2. Although the initial year 2 plan requires the testing of 56 cells only, 103 cells were purchased from an online vendor. Having additional cells serves three purposes: to strengthen the statistical analysis from the initial conditioning and characterization test (ICCT); to allow for potential outlier cells to be avoided; and finally, to provide comparable cells from the same batch for follow-up studies. Within this batch of cells, cells 001 to 102 were subjected to the ICCT test. Cell 103 was used to gather an accurate open circuit voltage (OCV) vs. state of charge (SOC) curve, and was then disassembled for half-cell testing.

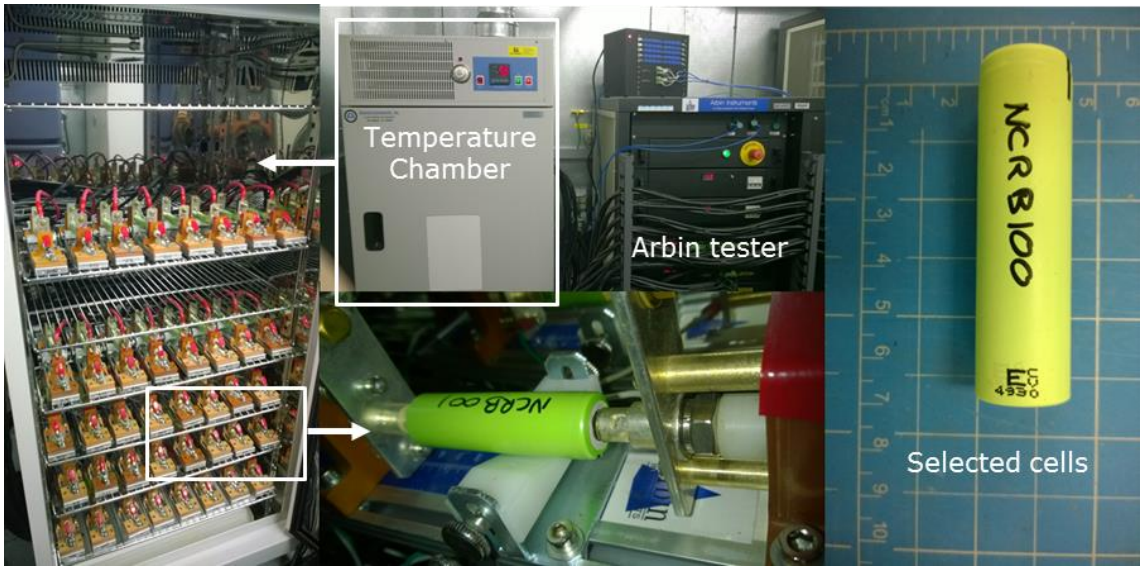

Figure 1: ARBIN LBT tester and temperature chamber (with battery holders installed) reserved for UTC project.

The disassembly of a cell from the batch is necessary to gather data from both electrodes in order to build an accurate cell model to enable accurate cell diagnosis and prognosis throughout the study. Upon disassembly, both electrode materials (positive and negative) were harvested and cycle-tested separately versus a metallic lithium reference electrode, in order to understand the individual electrochemical behavior of each electrode. The data is then used to construct a model of the cell, which is required at a later stage for diagnosis and prognosis purposes. This will be described in detail in a later report.

After completion of the ICCT test, cells 101 and 102 were used to validate the different aging protocols to be used in the main study [1]. These initial tests showcased some room for improvement in the model and corrective measures were implemented. Once the modified protocols were validated, the main experiment was launched with 36 cells. In parallel, the 4 remaining channels were used to condition cells for the calendar aging study [1].

The intent of this report is to describe results of the ICCT test; to present the improvements to the test protocols; and finally to provide an update on the testing status.

3 INITIAL CONDITIONING CHARACTERIZATION TEST (ICCT)

Before the start of any cycle-life evaluation, it is extremely important to identify and quantify the nature of cell-to-cell variations within a batch of cells. For this purpose, we designed an ICCT to which every cell of the batch was submitted before starting the main experiment. The capacities as well as the rest cell voltages (RCV) measured during this test are used to calculate the three parameters that are critical in determining the manufacturing variability in a batch of cells: the rate capability, the capacity ration and the resistance [2]:

Rate capability [unit-less] – The rate capability represents the cell's ability to deliver stored capacity when the discharge rate increases. In this study, it was calculated by dividing the capacity obtained at C/2 (discharge in 2 hours) by the capacity at C/5 (discharge in 5 hours).

Capacity ration [mAh / %SOC] – The term "capacity ration" is the capacity (Ah) obtained for each one percent of the SOC. It typically reflects the amount of active material in a cell. RCV measurements at the beginning of discharge (BOD) and the end of discharge (EOD) are used to derive a SOC range by interpolation of the maximum and minimum SOCs (e.g. 99.7 – 3.2 %). The capacity ration is then calculated by dividing the capacity returned during discharge by the SOC range variation.

Ohmic resistance [Ω] – The ohmic resistance consists of the contact resistance of the cell in the circuit and the conductive resistance of the cell (which primarily comes from the electrolyte). It is calculated using the initial voltage drop associated with the C/2 and C/5 discharges.

3.1 METHODOLOGY

The ICCT test consists of several cycles at C/2 until the capacity of the cell remains stable within 0.2% followed by 2 additional cycles at C/2 and C/5 with 4 hours rest before and after the discharges. All charges were performed using the manufacturer recommended conditions. The protocol is detailed in Appendix 1. Prior to the start of the ICCT test, the cells were weighed and their as-received open circuit voltage (OCV) was recorded.

In descriptive statistics, a box plot (Figure 2) is a convenient way of graphically depicting groups of numerical data through their quartiles. The box size is set to encompass 50% of the data. This is the interquartile range (IQR), the range between the 1st quartile (or lower quartile which splits the lowest 25% of the data from the highest 75%) and the 3rd quartile (or higher quartile which splits the lowest 75% of the data from the highest 25%). The whiskers extend to 1.5 times the IQR and any point outside can be considered as an outlier. The position of the median within the box gives additional information on the distribution: A centered median indicates a symmetric distribution. An un-centered median indicates an asymmetric distribution.

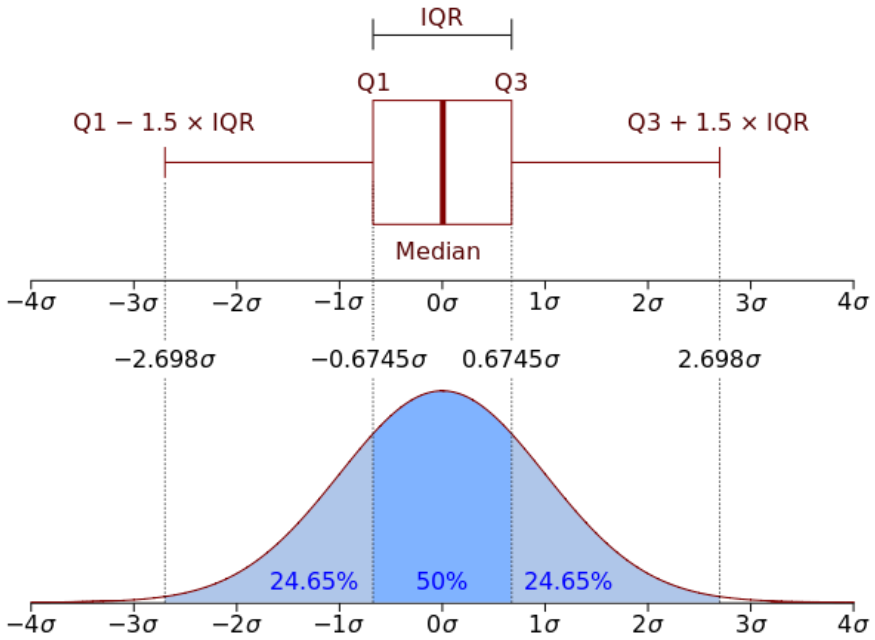

Figure 2: Box plot details compared to a normal distribution

The Q-Q plot is a graphical method used to compare two probability distributions by plotting their quantiles against each other. In our case, we compared the test results to a normal distribution and the quantile size was chosen so that every data point is plotted. The points plotted in a Q–Q plot are always non-decreasing when viewed from left to right. If the two distributions being compared are identical, the Q–Q plot follows a 45° line, y = x. Q–Q plots are often arced, or "S" shaped, indicating that the data distribution is more skewed than a normal distribution, or that it has heavier tails.

In the following section, most of the ICCT results will be split into quadrants: the top left quadrant displays the recorded values cell by cell, the top right quadrant shows the value distribution, the bottom left quadrant plots the associated box plot, and the bottom right quadrant the quantile-quantile (Q-Q) plot.

3.2 ICCT Results

Before analyzing the result of the ICCT test itself, Figure 3 presents the cells weight distribution. The average weight was 45.870g with 0.16% standard deviation. The weight distribution is close to normal since all the points sit on or close to the slope in the Q-Q plot. Nonetheless, it seems that the lower tail is larger than the upper tail (more deviation on the Q-Q plot and median not centered on the box plot). The box plot also shows one outlier, cell 020, which is slightly lighter (0.5g) than the rest of the batch.

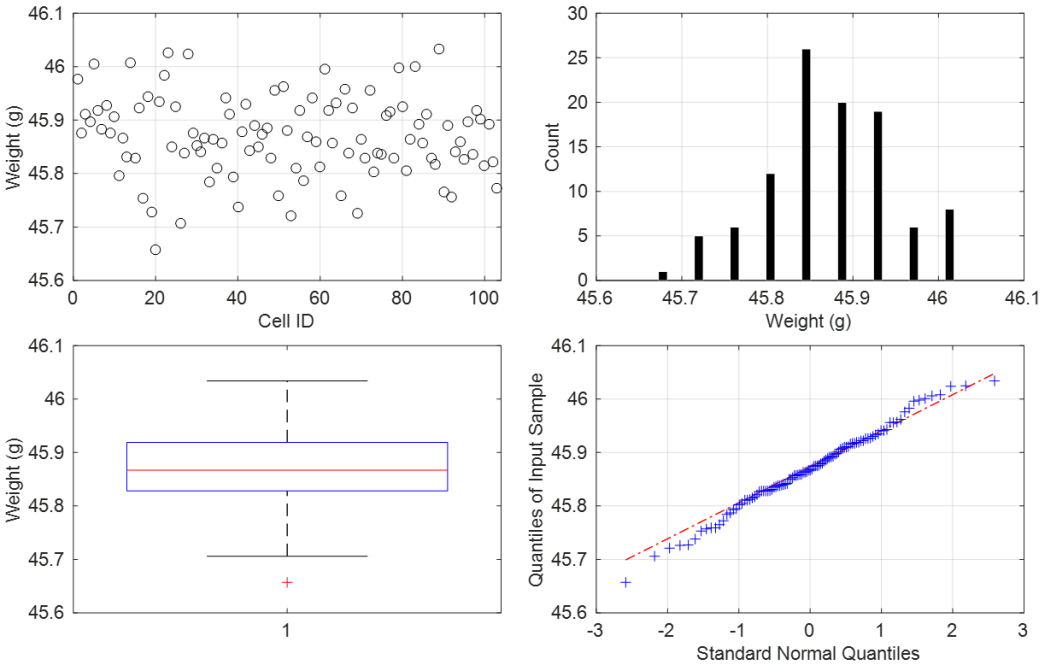

Figure 3: Weight repartition and associated statistics.

The second parameter to be checked prior to the analysis of the main ICCT test is the as-received OCV, Figure 4. The OCVs were measured prior to any testing on the cells with a NIST-traceable Keithley 2700 Source Meter Unit (SMU) over the course of 2 days. This 2 day span had an effect on the recorded value as there seems to be a 1mV difference in average OCV between the two days. This offset could originate from different equipment warm-up times (measurement error), or from a change in internal temperature of the lithium-ion cells. In any case, this apparent 1mV offset is not a significant source of error (0.02% standard variation).

The Q-Q plot showcases that the tails of the OCV distribution do not follow a normal distribution and that the distribution is asymmetric. Indeed, the lower values fell under the y = x slope which suggests that the lower OCVs are more dispersed than expected from a normal distribution. The higher values are also under the y = x slope which suggests that the upper tail is steeper than that of a normal distribution. Within the IQR, the distribution is normal as can be seen by the linear behavior on the Q-Q plot and the well centered median on the box plot. Finally, the box plot also shows 2 outliers, cells 005 & 006, which had lower as-received OCVs.

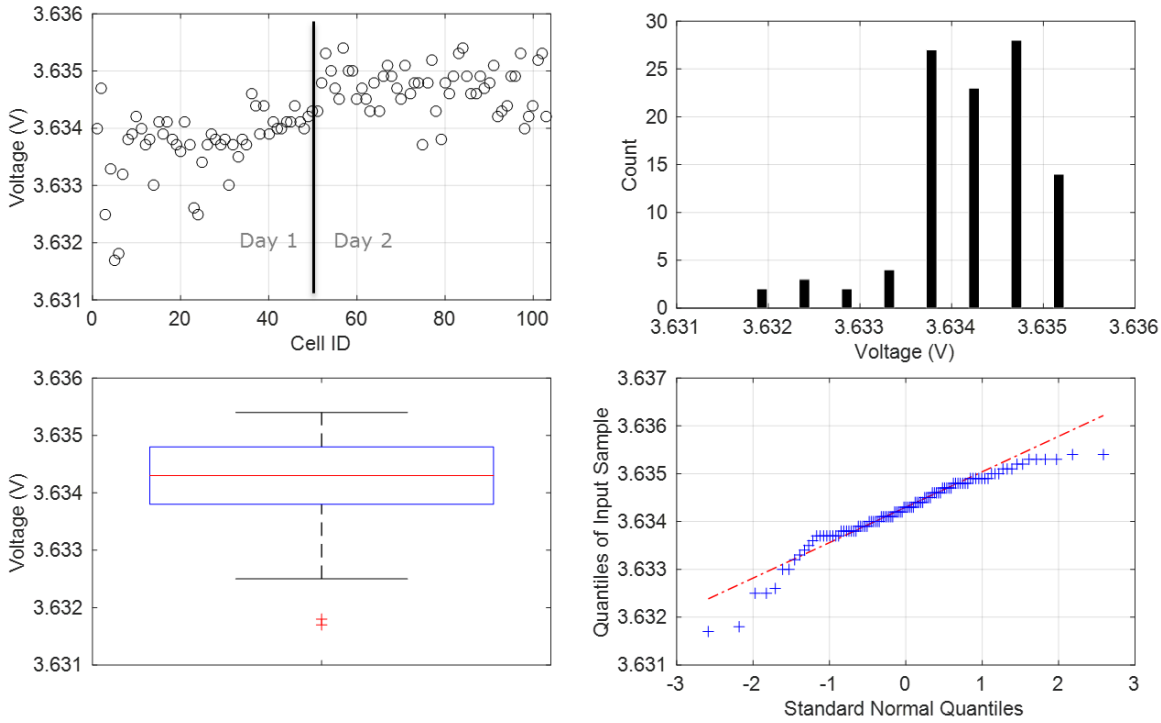

Figure 4: As-received OCV repartition and associated statistics.

The recorded OCVs were translated into SOCs using an OCV=ƒ(SOC) curve inferred from the testing of cell 103, Figure 5. The OCV=ƒ(SOC) was obtained by averaging the electrochemical response of the cell at C/25 in the charge and discharge regimes. The obtained curve is presented in Figure 6. The average calculated SOC was 46.57% with a 0.27% standard deviation. The standard deviation of the SOC distribution is much higher than that of the OCV because the voltage response of the cell around 3.6V (circle on Figure 6) is fairly flat. This implies that a small voltage variation can introduce a significant SOC variation. The maximum recorded SOC was 44.76% and the minimum 44.15%, a 0.6% difference. According to the box plot, and similarly to the OCV distribution, cells 005 & 006 appear to have a lower SOC when received. The origin of the lower SOC of cells 005 & 006 is unknown but it cannot be, at any rate, considered a significant variation.

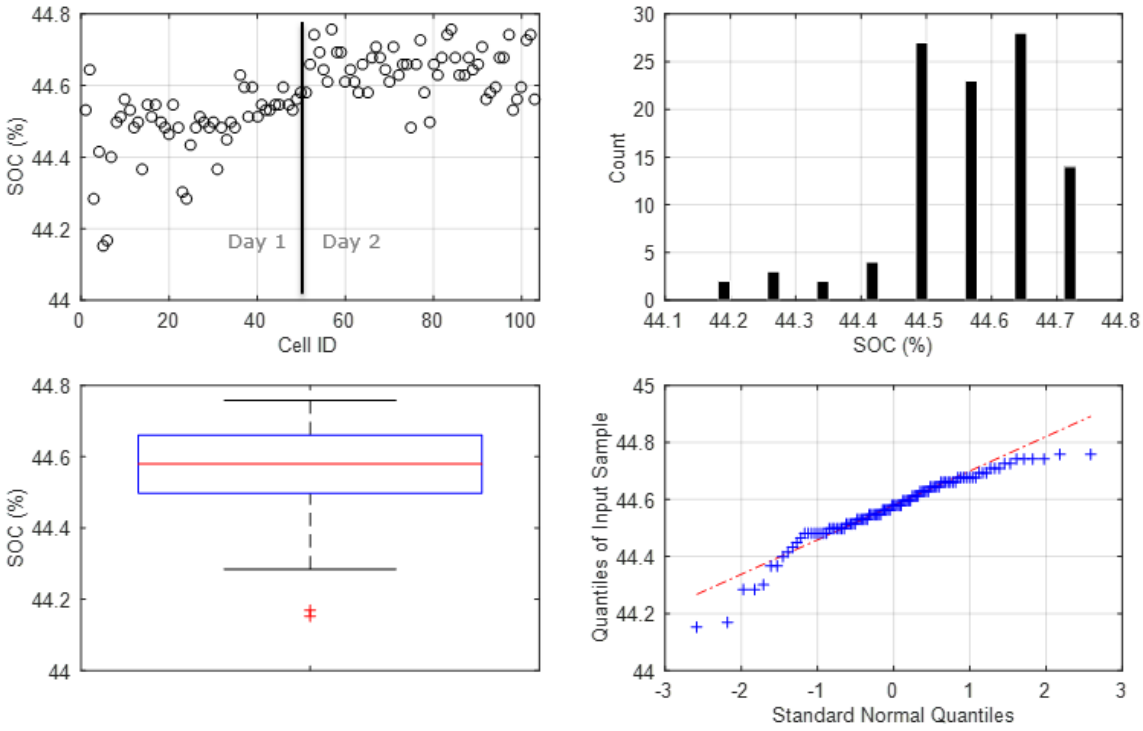

Figure 5: As-received SOC distribution and associated statistics.

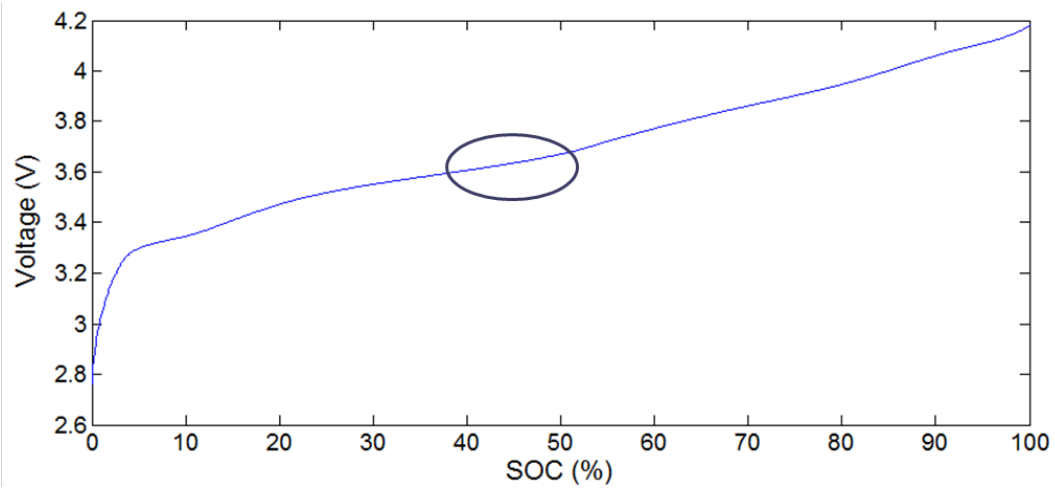

Figure 6: NCR18650B OCV=f(SOC) function.

The observed variations in as-received SOC for cells 005 and 006 does not necessarily imply that they are bad cells. Nonetheless, recording these variations is important if the cells are to be used in modules. Indeed, the cells to be installed in a module are sometimes selected only from their as-received OCVs. Therefore looking at its variation and the corresponding SOC variation gives practical information on the maximum SOC imbalance to be expected in modules containing these cells. This information will likely prove to be valuable in follow-up studies if module modeling/testing is considered.

The next parameter to investigate is the ohmic resistance. As mentioned in the introductory section, it is calculated from the voltage drop induced by the application of current at the beginning of both the low rate and the high rate discharges. Figure 7 presents the results of the resistance calculation on the entire batch. The average resistance was 59.6 mΩ with 2.95% standard variation. As can be seen from the top right quadrant and the Q-Q plot, the distribution is asymmetric with a short tail for lower resistance and a large tail for the higher resistance. Also, from the box plot, there were 3 clear outliers (032, 055 and 067) with a much higher resistance than of the other cells from the batch.

This distribution shape was expected since it is hard to reduce the resistance but extremely easy to increase it (i.e. any contact issue will significantly increase the resistance). An example of the influence of the contact on the resistance can be seen by looking closely at the top left quadrant: the average resistance seems to slightly increase with the cell number. This can be explained by the fact that our battery holders have a copper foam to ensure maximum contact and that this foam oxidizes with time. Since we had to test 102 cells on a 40 channel machine, the ICCT test was done in 3 rounds (001-040, 041-080 and 081-102). Figure 8 presents the distribution and the box plots for the 3 rounds. Although the distributions are similar, the average and median values seem to slightly increase (by less than .75mΩ or 1.25%) from round to round as a result of the gradual oxidation of the battery holder's conductive foam. This increase is well within the standard deviation of the resistance values and is thus negligible. To remedy this gradual increase in contact resistance, we elected to sand the holder's contacts and apply an anti-oxidant compound (Ox-Gard, by Gardner Bender) onto the copper foam pads. This fix should help maintain a stable contact resistance throughout testing. We'll continue to monitor the situation.

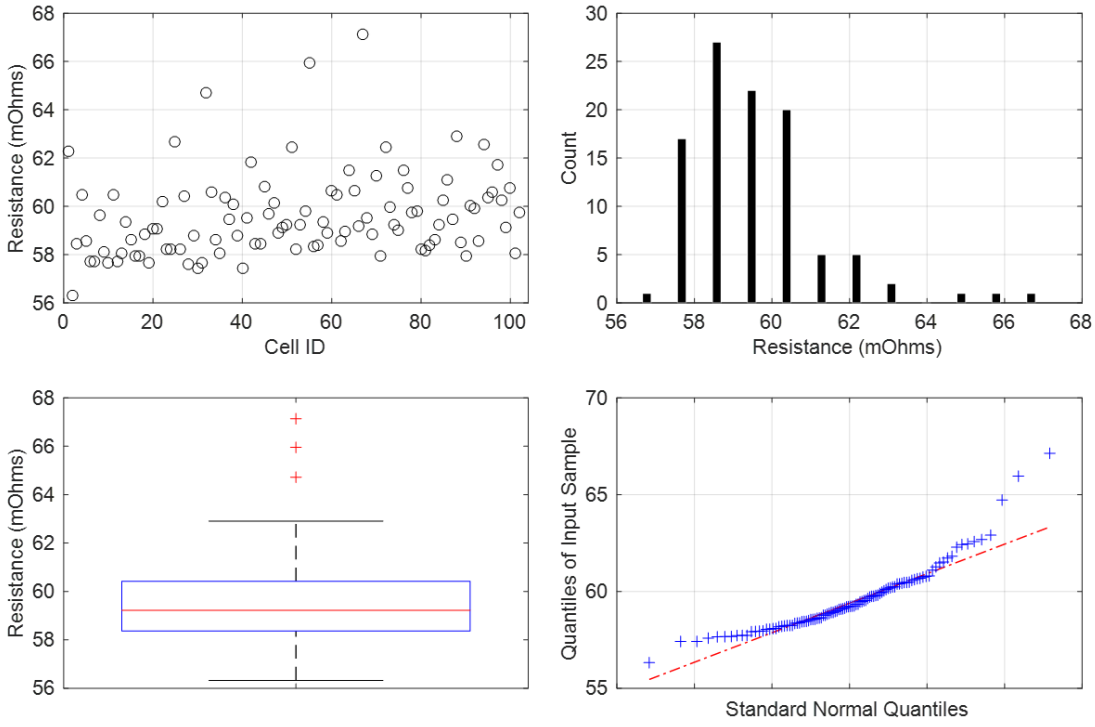

Figure 7: Ohmic resistance distribution and associated statistics.

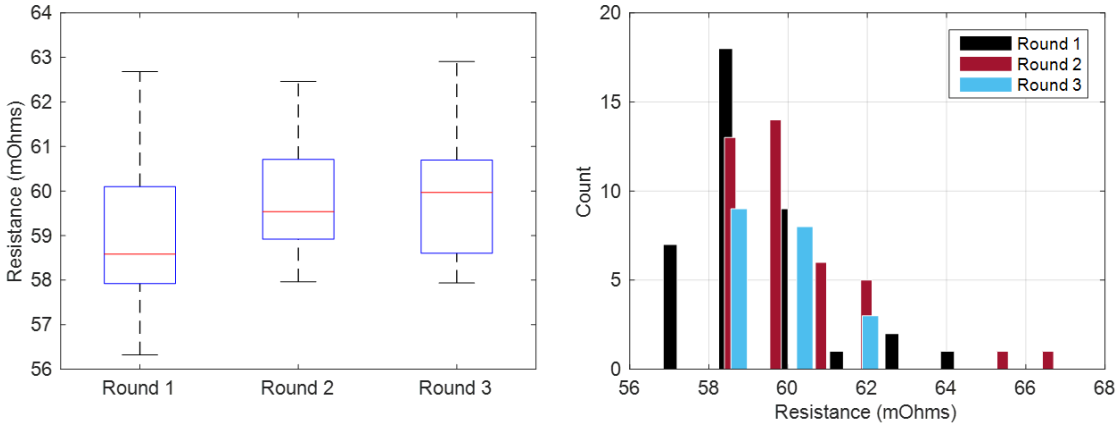

Figure 8: Box plot and distribution for the 3 batches of resistance measurements.

The next parameters to be screened are the capacities recorded during the two discharges at C/5 (low rate) and C/2 (high rate), Figure 9. These capacities will be used to calculate the rate capability, the second attribute that characterizes the cell-to-cell variations within a batch of cells. The cells delivered 3.269 Ah in average at a C/5 rate and 3.177 Ah at a C/2 rate with standard deviations below 1%. The standard deviation of the C/2 discharges is slightly higher (0.8% vs. 0.6%) and this explains the different slopes on Figure 9d. Both capacity distributions are normal and, from the boxplots, there are two outliers with higher capacities under C/5 discharge (cells 014 & 099) and one under C/2 discharge (cell 014).

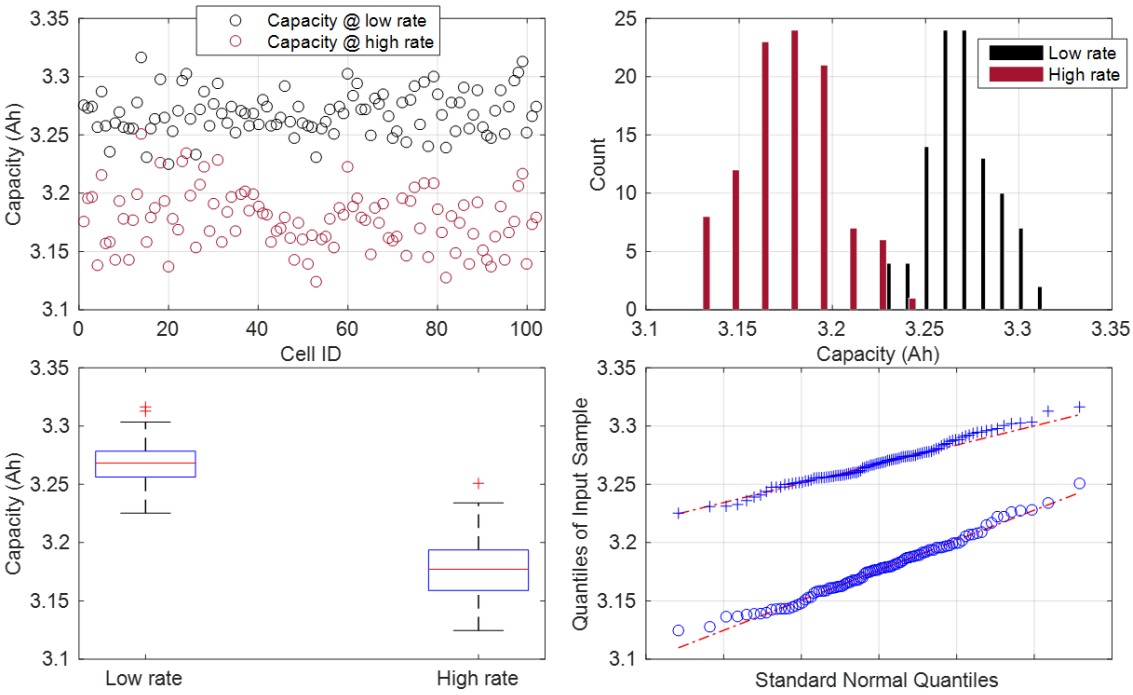

Figure 9: C/5 and C/2 capacity distribution and associated statistics.

A ratio of the capacity values at C/5 and C/2 can be used to derive the cells rate capability, Figure 10. The average rate capability is 97.20 with 0.50% standard deviation. Although there are no outliers, the rate capability seems to decrease with the cell number which suggests that the aforementioned increase of resistance with the testing rounds played a role in lowering the C/2 capacity and this will be discussed in the next section. The distribution is not normal and has pretty steep tails as shown by the variations to the y = x slope for both the low-end and high-end values in the Q-Q plot.

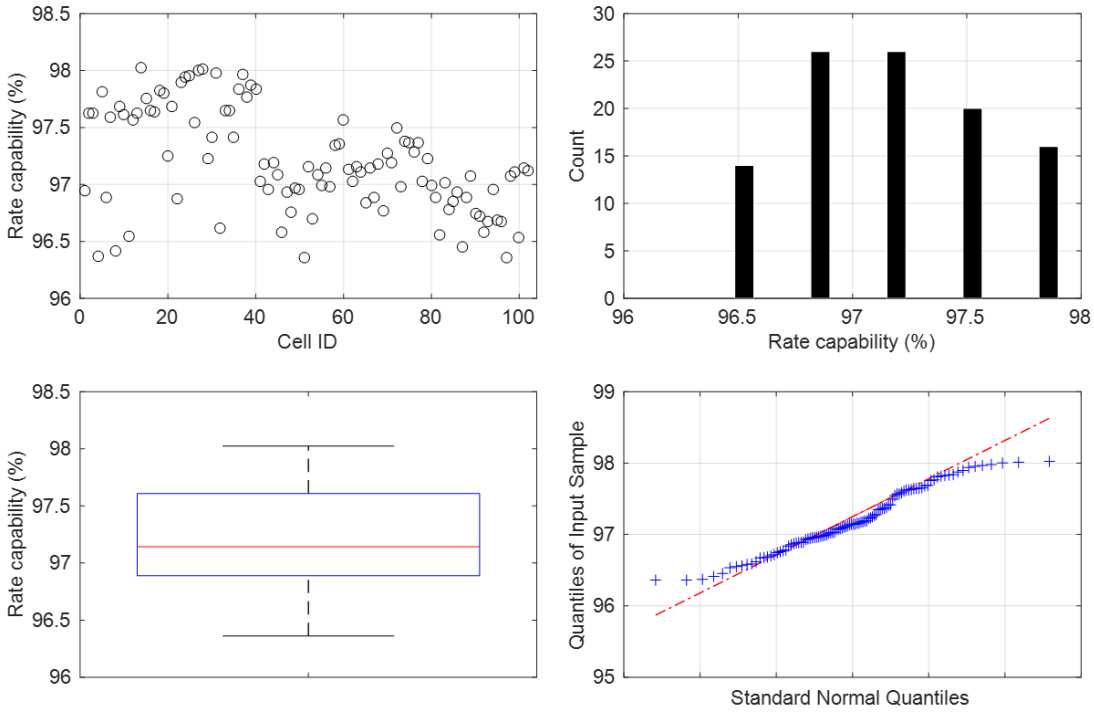

Figure 10: Rate capability distribution and associated statistics.

The last parameter to consider is the capacity ration, Figure 11, which is inferred from the SOC calculated from the rest cell voltages at the beginning and end of each discharge. The average capacity ration is 3.425 Ah/%SOC with 0.38% standard variation. This suggests that the cells could deliver at most 3.425Ah under ideal conditions (i.e. very slow charging/discharging), which is above their rated capacity. The observed distribution is close to normal (see Q-Q plot) and is symmetric (median in the center of the box plot).

The results obtained throughout the entire ICCT are summarized in Table 1. It has to be noted that cells 005 & 006 that had an abnormally low initial SOC were not outliers in the second stage of the testing, they are therefore considered acceptable to use.

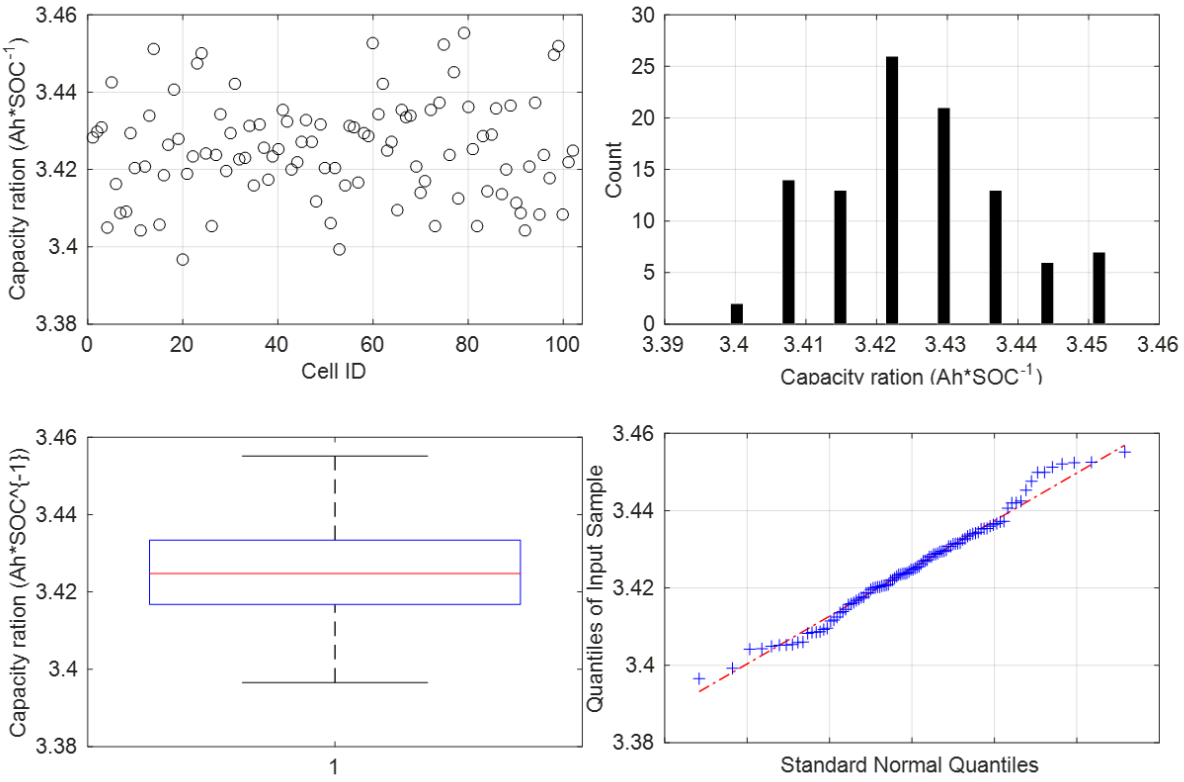

Figure 11: Capacity ration distribution and associated statistics.

Table 1: ICCT test summary.

	Mean	Median	Std. deviation (%)	Min	Max	Lower quartile	Upper quartile
Cell weight (g)	45.870	45.867	*0.16*	45.657	46.034	45.828	45.919
Initial OCV (V)	3.634	3.634	*0.02*	3.632	3.635	3.634	3.635
Initial SOC (%)	44.57	44.58	*0.27*	44.15	44.76	44.50	44.66
Ohmic resistance (mΩ)	**59.6**	**59.2**	***2.95***	**56.3**	**67.1**	**58.4**	**60.4**
C/5 capacity (Ah)	3.269	3.268	*0.56*	3.225	3.316	3.256	3.278
C/2 capacity (Ah)	3.177	3.177	*0.8*	3.125	3.251	3.159	3.194
Rate capability	**97.20**	**97.14**	***0.46***	**96.36**	**98.02**	**96.89**	**97.61**
C/5 BOD RCV (V)	4.174	4.173	*0.04*	4.172	4.189	4.173	4.174
C/5 EOD RCV (V)	3.231	3.233	*0.41*	3.189	3.259	3.223	3.241
C/2 BOD RCV (V)	4.173	4.173	*0.04*	4.172	4.190	4.173	4.174
C/2 EOD RCV (V)	3.314	3.314	*0.14*	3.297	3.321	3.311	3.317
Capacity ration (mAh/%SOC)	**3.425**	**3.425**	***0.38***	**3.397**	**3.455**	**3.417**	**3.433**

3.3 ICCT ANALYSIS: ATTRIBUTES OF CELL-TO-CELL VARIATIONS

As described in our previous study [2], the three attributes that can be used to quantify the cell-to-cell variations are the ohmic resistance, the rate capability and the capacity ration (Table 1, in bold) The standard deviations for these three parameters are 2.95%, 0.46% and 0.38% respectively. Compared to published values for other batches of cells, these standard deviation values are rather small [2, 3]. The cells are therefore highly consistent (high quality of manufacturing) and ideal for the study to be undertaken.

Looking at cell selection, a 3D box plot with those three parameters (Figure 12) showcases that only three cells seem to be outliers (in red) and only in terms of ohmic resistance: cells 032, 055 and 067.

As we suspect these high resistances might be associated with contact problems. We believe these cells can still be used for experiments where several cells are tested under the same conditions but their usage should be avoided until no other cells are available. The cell selection for the main aging study and the calendar aging study is presented in section 5.

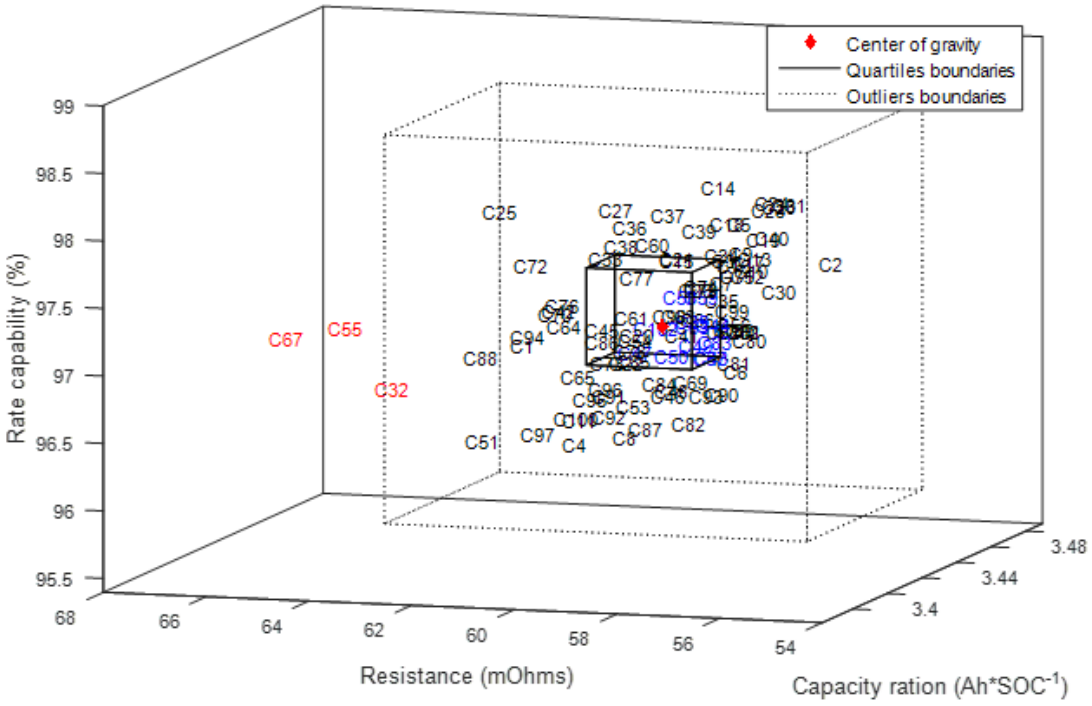

Figure 12: Cell-to-cell variation 3D box plot.

Figure 13 presents a correlation analysis on the 3 attributes of cell-to-cell variations. There are several correlation coefficients, often denoted by the Greek letter ρ, measuring the degree of correlation. The most common of these is the Pearson correlation coefficient, which is sensitive only to a linear relationship between two variables. This coefficient is obtained by dividing the covariance of the two variables by the product of their standard deviations. The Pearson correlation is +1 in the case of a perfect direct (increasing) linear relationship (correlation), −1 in the case of a perfect decreasing (inverse) linear

relationship, and some value between −1 and 1 in all other cases, indicating the degree of linear dependence between the variables. As it approaches zero there is less of a relationship (closer to uncorrelated). The closer the coefficient is to either −1 or 1, the stronger the correlation between the variables. Additionally, the p-values were calculated for each correlation. P-values were calculated to test the hypothesis of no correlation against the alternative that there is a nonzero correlation. If the p-value is small, say less than 0.05, then the correlation is significantly different from zero. The results of this analysis are compiled in Table 2.

There is no correlation between the capacity ration and the resistance (low ρ and high p-value) but there seems to be a correlation between the resistance and the rate capability and between the rate capability and the capacity ration (both have medium ρ and low p-value). Both the no-correlation between capacity ration and resistance and the correlation between resistance and rate capability were expected: capacity ration reflects the thermodynamic maximum capacity and should be unaffected by kinetics; also a higher resistance is likely to lower the capacity available at high rates and thus impact the rate capability. The last one, rate capability vs. capacity ration, is intriguing since it was found that cells with a high capacity ration are likely to also have a high rate capability. Higher capacity ration is thought to originate from 2 sources: longer jelly roll or heterogeneities in additive content. Under the first scenario, local current density is lowered (same current applied but more surface) with higher capacity rations which could in return improve the rate capability. Under the second scenario, the rate capability should decrease for high capacity rations the additional capacity is induced by a lower additive to active material ratio and thus less power ability. In our case, given the observed direct correlation, we are more likely to experience the case where electrodes are uniform across cells but of slightly different lengths from one cell to another.

Table 2: Correlation analysis results for cell-to-cell variations attributes.

	r^2	ρ	p-value
Capacity ration vs. Resistance	0.011	0.012	0.907
Resistance vs. Rate capability	0.112	-0.335	0.001
Rate capability vs. Capacity ration	0.179	0.423	0.000

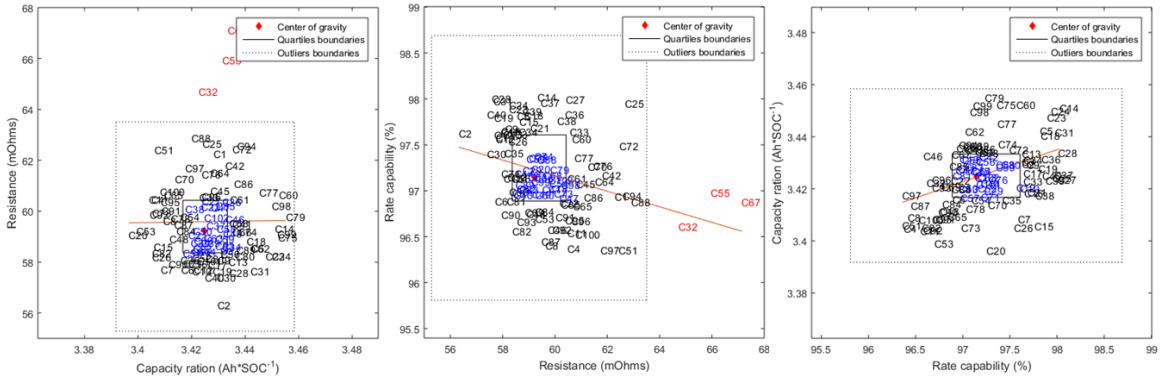

Figure 13: Correlation analysis for the 3 attributes to cell-to-cell variations.

Cell selection can become an important issue if module testing is needed. Depending on the number of cells to be assembled, it might be impractical to perform the full ICCT test on all of them. To circumvent this issue, we can look into possible correlations between the cells' weight and initial SOC, which are easily measureable and the three attributes to the cell-to-cell variations, Table 3 and Figure 14.

For capacity ration, the best correlation is found with the cells' weight (medium ρ and low p-value). In our previous study, [2], we found no correlation between weight and capacity ration but the tested cells had half the energy density of the cells selected in this study.

For the resistance and the rate capability, the best correlation is found with the initial SOC.

This analysis shows that cell selection without ICCT is possible by matching the cell weight and initial SOC, although not recommended since the correlation coefficients are all below 0.5 and thus, barely correlated.

Table 3: Correlation analysis results for cell-to-cell variation attributes vs. initial parameters.

	r^2	ρ	p-value
Rate capability vs. Weight	0.016	0.125	0.211
Capacity ration vs. Weight	0.221	0.470	0.000
Resistance vs. Weight	0.011	0.105	0.292
Rate capability vs. initial SOC	0.180	0.424	0.000
Capacity ration vs. initial SOC	0.032	-0.179	0.072
Resistance vs. initial SOC	0.051	0.225	0.022

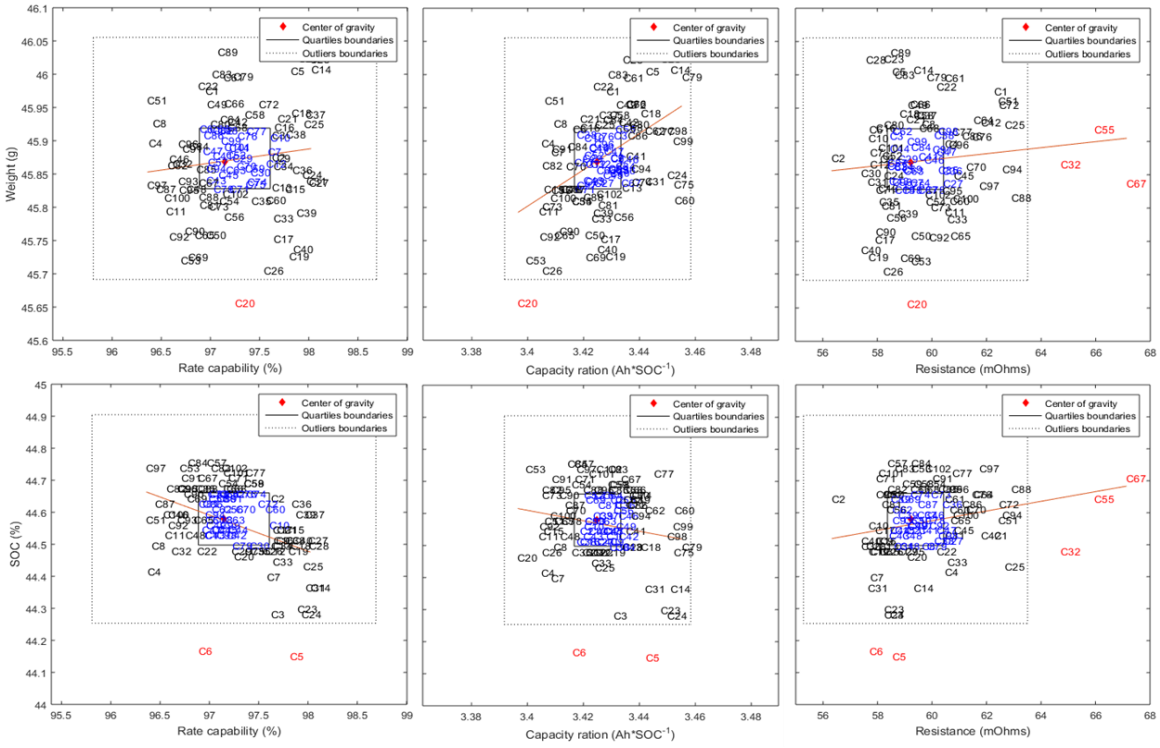

Figure 14: Correlation analysis between weigh, SOC and cell-to-cell variations attributes.

4 PRELIMINARY TESTING AND TESTING PLAN REFINEMENTS

4.1 SCALING OF REAL VEHICLE DATA

As mentioned in our previous report [1], we are planning to use the current data from an average commute driving cycle extracted from our database of vehicle driving data throughout this round of testing. In order to determine the scaling factor that needs to be used to adapt the vehicle data to the Panasonic cells, we need to calculate the Battery Size Factor (BSF). The method to determine the BSF is given in the Battery Test Manual For Plug-In Hybrid Electric Vehicles [4]. In this publication, the BSF is defined as:

"Battery Size Factor (BSF) – for a particular cell or module design, an integer which is the minimum number of cells or modules expected to be required to meet all the performance and life targets. If this value cannot be determined prior to testing, the Battery Size Factor is chosen as the minimum number of cells or modules that can both satisfy the charge sustaining energy target with a 30% power margin and provide a 30% energy margin for Charge Depleting Available Energy at beginning-of-life."

In our case, we can consider the performance target to be the vehicle battery pack capacity and therefore calculate the BSF directly without the need for margins. We can then calculate the BSF by comparing the capacity of our cells to the capacity of the battery pack that was installed in the cars. The battery packs in the vehicles were 95 Ah batteries [5]. The Panasonic cells considered for this work being 3.2 Ah (*cf.* spec sheet in appendix 2), we would need 30 of them in parallel to match the 95 Ah capacity of the battery pack. As a result, a BSF of 30 will be considered for this work and the currents from the vehicle data will be divided by 30 to be deemed applicable to our single cell.

After scaling of the selected vehicle data, the average current of the single cells is -1C in discharge and C/4 in charge, with maximums at -2.5C and 1C in discharge and charge respectively (cf. Appendix 3). This is well within the recommended usage of the selected single cell. The two selected commute trips from the vehicle driving data will each utilize about 0.42 Ah out of the cell which represents about 7.5% of the cell's rated capacity.

4.2 TEST ACCELERATION

The timing proposed in the previous report (*cf.* fig 7 in [1], repeated below, Figure 15) accounted for full charges at each of the charging steps and the full schedule was set to last about 16 hours. With the capacity to be used driving each day calculated as 2 x 7.5%, we can now estimate a tighter schedule to accelerate the testing further. Indeed, starting from a fully charged state, the cell will discharge around 7.5% of its capacity during the first leg of driving. The first driving step can be followed by the V2G step that is set to last 1 hour at a P/4 power which will discharge another 25 to 30% of the cell capacity. This suggests that the cell will not be more than 50% discharged in this experiment when the charge starts. The charge will then likely last less than half of the time made available for charging. Therefore reducing the time devoted to the charge from 4 hours to 2.5 hours will allow the test to be significantly sped up while leaving some room for an eventual increase of the CV step after aging. With a 30 min rest in the schedule to better match the reality of the vehicle driving data (5 min before V2G and 25 min after the charge), the maximum duration of this step can be cut to 4 hours instead of the 5.5 hours documented in [1].

Using the same approach, we can calculate that for the second stage, the cell will already be more than 50% charged also (worst case: 2 x 7.5% for driving + 25 - 30% of V2G). The slower charge should therefore last no more than 4 hours out of the 8 hours planned. Adding 30 minutes to make sure the charge is completed, the total duration of this second stage could then be 6 hours instead of 9.5 hours.

With these iterations, the testing time is reduced from 16 hours to 11 hours for 1 cycle, Figure 16. This allows 20 more cycles to be performed per month. In total we will be testing the impact of 65 "days" in 30 days, a > x2 acceleration compared to real life.

In order to make sure that the test will stay in sync, all steps will be time limited. It has to be noted that 5 minutes of the 30 minutes rest times were shifted to after the driving and to after an eventual V2G discharge. This is to mimic the time it takes to plug the car and enter information in the charger.

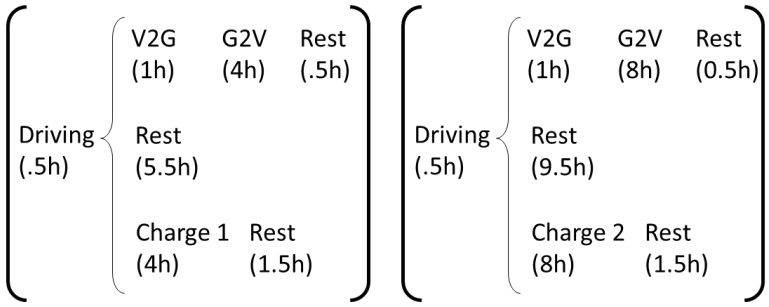

Figure 15: Test duration from [1].

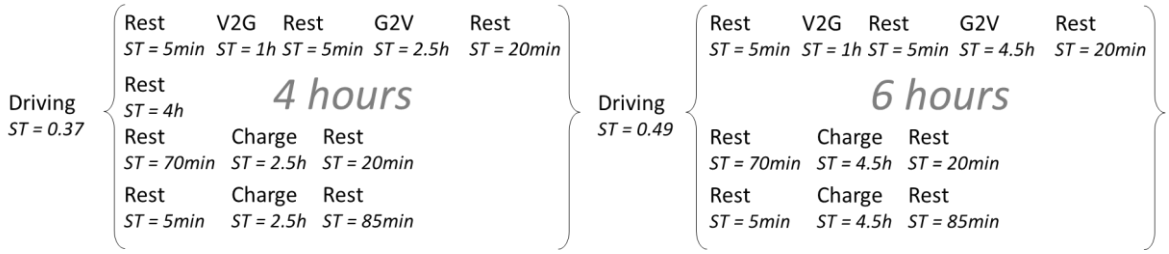

Figure 16: Test duration and step limit for actual experiment.

Finally, the charging cutoff voltage was set to 4.1 V instead of 4.2 V. After some research, it appeared that 4.1 V is the cutoff voltage used in vehicle applications. Indeed, a similar model of lithium-ion cells has been reported to be used in Tesla Motors' line of vehicles. In particular, it is believed that the Model S (2012-15) employs a variation of the NCR18650 cell family, featuring a common chemistry with the NCR18650B cell. To prolong the battery pack lifetime (calendar and cycle aging) of these vehicles, an engineering decision has been made to use a charge voltage lower than the recommended 4.2 V value (Appendix 2). In "Standard Charge" mode, the cell voltage is limited to 4.1 V at the end of charge. In "Max Range" mode however, the cell voltage is limited to 4.2 V [6][7][8]. The repeated use of "Max Range" charge mode is discouraged by the owner's manual as it is detrimental to the battery pack long-term performance (faster degradation). Since this study is meant to determine the effect of V2G and not the impact of "max range" / "standard range", we will use 4.1 V as the cutoff voltage for the aging study.

4.3 CALENDAR AGING MATRIX

The calendar aging matrix was also improved compared to the one proposed in [1] by using more realistic SOC values for the 100% and 0% SOC conditions. The 100% SOC condition was replaced with a 99% condition which corresponds to the OCV after a 4.2V charge, in accordance with the "Max Range" option described above. The 0% SOC condition was changed to 6% to mimic the SOC at the end of a C/2 discharge where the cell is considered completely discharged under standard conditions.

The final matrix is presented in Figure 17:

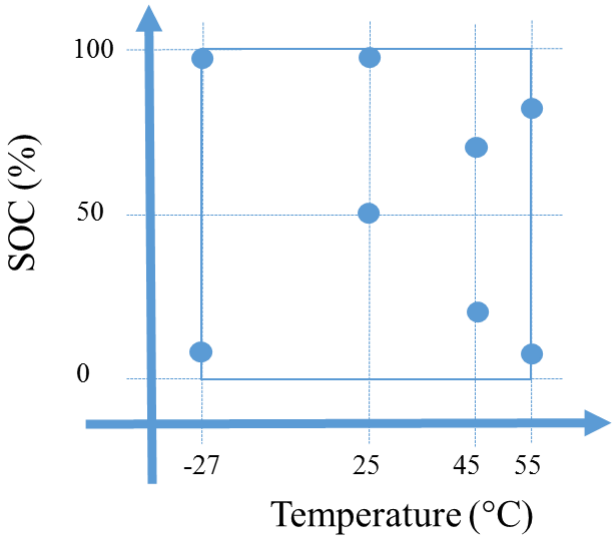

Figure 17: Updated calendar aging test matrix.

5 TEST STATUS

As of June 30th 2015, the cells performing the cycling experiment cycled 90 times and are currently starting their second reference performance test (RPT). The cells performing calendar aging aged between 2 and 5 weeks. The first set of cells (038, 039, 043 and 044) is set to perform their second RPT in the coming week. The detailed test status is presented in **Error! Reference source not found.**.

Table 4: Test status as of June 30th 2015.

Main experiment

Cell #	Aging type*	ICCT	As of June 30th 2015	
			RPT	EQ. Days
NCRB001	DCR-DCR	✓	1	90
NCRB002	DCR-DCR	✓	1	90
NCRB003	DCR-DCR	✓	1	90
NCRB004	DCR-CR	✓	1	90
NCRB005	DCR-CR	✓	1	90
NCRB006	DCR-CR	✓	1	90
NCRB007	DCR-RC	✓	1	90
NCRB008	DCR-RC	✓	1	90
NCRB009	DCR-RC	✓	1	90
NCRB010	CR-DCR	✓	1	90
NCRB011	CR-DCR	✓	1	90
NCRB012	CR-DCR	✓	1	90
NCRB013	CR-CR	✓	1	90
NCRB014	CR-CR	✓	1	90
NCRB015	CR-CR	✓	1	90
NCRB016	CR-RC	✓	1	90
NCRB017	CR-RC	✓	1	90
NCRB018	CR-RC	✓	1	90
NCRB019	RC-DCR	✓	1	90
NCRB020	RC-DCR	✓	1	90
NCRB021	RC-DCR	✓	1	90
NCRB022	RC-CR	✓	1	90
NCRB023	RC-CR	✓	1	90
NCRB024	RC-CR	✓	1	90
NCRB025	RC-RC	✓	1	90
NCRB026	RC-RC	✓	1	90
NCRB027	RC-RC	✓	1	90
NCRB028	R-DCR	✓	1	90
NCRB029	R-DCR	✓	1	90
NCRB030	R-DCR	✓	1	90
NCRB031	R-CR	✓	1	90
NCRB033	R-CR	✓	1	90
NCRB034	R-CR	✓	1	90
NCRB035	R-RC	✓	1	90
NCRB036	R-RC	✓	1	90
NCRB037	R-RC	✓	1	90

Calendar aging

Cell #	Aging type	ICCT	As of June 30th 2015	
			RPT	AGING
NCRB038	-27°C|99% SOC	✓	1	5 weeks
NCRB039	-27°C|99% SOC	✓	1	5 weeks
NCRB043	-27°C|06% SOC	✓	1	5 weeks
NCRB044	-27°C|06% SOC	✓	1	5 weeks
NCRB046	25°C|50% SOC	✓	1	4 weeks
NCRB047	25°C|50% SOC	✓	1	4 weeks
NCRB049	25°C|100% SOC	✓	1	4 weeks
NCRB050	25°C|100% SOC	✓	1	4 weeks
NCRB056	45°C|20% SOC	✓	1	3 weeks
NCRB058	45°C|20% SOC	✓	1	3 weeks
NCRB059	45°C|70% SOC	✓	1	3 weeks
NCBR063	45°C|70% SOC	✓	1	3 weeks
NCRB069	55°C|81.5% SOC	✓	1	2 weeks
NCRB083	55°C|81.5% SOC	✓	1	2 weeks
NCRB085	55°C|06% SOC	✓	1	2 weeks
NCRB093	55°C|06% SOC	✓	1	2 weeks

*D: P/4 discharge
C: Charge
R: Rest

6 CONCLUSIONS

In conclusion, we completed the ICCT and verified that the cells offer a high level of consistency and are therefore well suited for this study. The three attributes of cell-to-cell variation, namely the ohmic resistance, the rate capability, and the capacity ration have standard deviations of only 2.95%, 0.46% and 0.38% respectively. Compared to published values for other batches of commercial cells, these values are rather small.

Among the 100-cell batch, we carefully selected 16 cells for the calendar aging study. Since a small number of cells are subjected to the calendar aging test, these cells were selected on the basis of their very high consistency (located within the quartiles boundaries for each of the three attributes of cell-to-cell variations). We selected another 36 cells for the cycle-aging study. The selection criterion for the cycle-aging study were slightly loosened since a larger number of samples is required for the cycle-aging study as compared to the calendar aging (i.e. 2 samples for calendar aging vs. 3 samples for each cycle-aging test condition). Overall, all 52 cells are well within the outlier boundaries (i.e. none of them can be considered an outlier), see Figure 18.

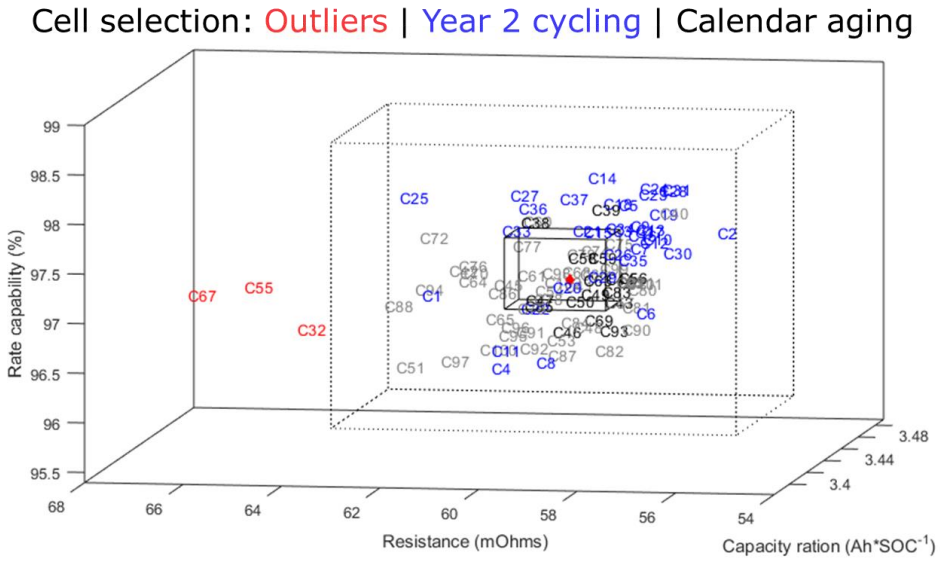

Figure 18: Cell selection based on ICCT results.

After completion of the ICCT, we used a couple of spare cells to check that the test protocols that we implemented worked as intended. The 12 variations of V2G schedule running on the Arbin battery tester have been proof-tested. After minor corrections, satisfactory results have been achieved and we determined that we could safely proceed with launching the main experiment

The testing is in progress and is running according to plan. The cells cycled more than 90 times already and are currently performing an RPT to assess their electrochemical behavior after this first leg of aging. The cells undergoing calendar aging are also scheduled to perform their first RPT in the coming weeks.

The next report will highlight the results gathered from these initial RPTs.

7 ACKNOWLEDGEMENTS

This report was funded under a subaward to the Hawaii Natural Energy Institute, University of Hawaii at Mānoa, from the Florida Solar Energy Center, University of Central Florida, through a grant from the US Department of Transportation's University Transportation Centers Program, Research and Innovative Technology Administration.

8 REFERENCES

[1] Dubarry M. "Test Plan to Assess Electric Vehicle Cell Degradation under Electric Utility Grid Operations", *EVTC Report HNEI-03-15*, pp. 1-14, (2015).
[2] Dubarry M., Vuillaume N., Liaw B. Y. "Origins and accommodation of cell variations in Li-ion battery pack modeling", *Int J Energ Res* 34, pp. 216-31, (2010).
[3] Dubarry M., Truchot C., Cugnet M., Liaw B. Y., Gering K., Sazhin S., et al. "Evaluation of commercial lithium-ion cells based on composite positive electrode for plug-in hybrid electric vehicle applications. Part I: Initial characterizations", *J Power Sources* 196, pp. 10328-35, (2011).
[4] INL. "Battery Test Manual For Plug-In Hybrid Electric Vehicles", *USDOE Report INL/EXT-07-12536*, pp. 1-67, (2008).
[5] Dubarry M., Bonnet M., Dailliez B., Teeters A., Liaw B. Y. "Analysis of Electric Vehicle Usage of a Hyundai Santa Fe Fleet in Hawaii", *Journal of Asian Electric Vehicles* 3, pp. 657-63, (2005).
[6] http://www.teslamotorsclub.com/showthread.php/21850-NHTSA-Opened-Up-the-Model-S-Battery-Pack-Pics/
[7] http://teslatap.com/undocumented/
[8] http://www.teslamotorsclub.com/showthread.php/22341-Model-S-Battery-Voltage

APPENDIX

1. CONDITIONING PROCEDURE

	#	Type	Control	Limits	Sampling rate!
PART 1	01	Rest	10 seconds		2s
	02	Charge	@ recommended CC-CV	Recommended charge voltage* & cutoff current**	3.6s or 2mV
	03	Discharge	@ C/2	Recommended discharge voltage	3.6s or 2mV
	04	Loop	Go back to [02] (Charge)	Twice (for 3 cycles)	
	05	*Decision*	*Continue if*	*$(Q_{n-1}-Q_n)/Q_n \leq 0.2\%$, otherwise repeat [02-04]*	
PART 2	06	Charge	@ recommended CC-CV	Recommended charge voltage & cutoff current	3.6s or 2mV
	07	Rest	4 hours***		5min
	08	Discharge	@ C/5	Recommended discharge voltage	9s or 2mV
	09	Rest	4 hours***		5min
	10	Charge	@ recommended CC-CV	Recommended charge voltage & cutoff current	3.6s or 2mV
	11	Rest	4 hours***		5min
	12	Discharge	@ C/2	Recommended discharge voltage	3.6s or 2mV
	13	Rest	4 hours***		5min
	14	Charge	@ recommended CC-CV	To 50% capacity for storage	3.6s or 2mV

! Record last data point of each step as well.

* 4.2V for the Panasonic NCRB (cf. Appendix 2).

** C/50 (65mA) for the Panasonic NCRB (cf. Appendix 2).

*** If time permits, longer rest periods are preferred (e.g. 8 hours), for every step of both formation and RPT.

2. PANASONIC NCRB18650B SPECIFICATION SHEET

Panasonic

Lithium Ion

NCR18650B

Features & Benefits

- High energy density
- Long stable power and long run time
- Ideal for notebook PCs, boosters, portable devices, etc.

*At temperatures below 10°C, charge at a 0.25C rate.

Specifications

Rated capacity[1]	Min. 3200mAh
Capacity[2]	Min. 3250mAh Typ. 3350mAh
Nominal voltage	3.6V
Charging	CC-CV, Std. 1625mA, 4.20V, 4.0 hrs
Weight (max.)	48.5 g
Temperature	Charge*: 0 to +45°C Discharge: -20 to +60°C Storage: -20 to +50°C
Energy density[3]	Volumetric: 676 Wh/l Gravimetric: 243 Wh/kg

[1] At 20°C [2] At 25°C [3] Energy density based on bare cell dimensions

Dimensions

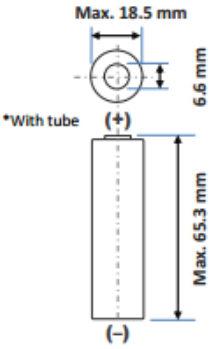

For Reference Only

Charge Characteristics

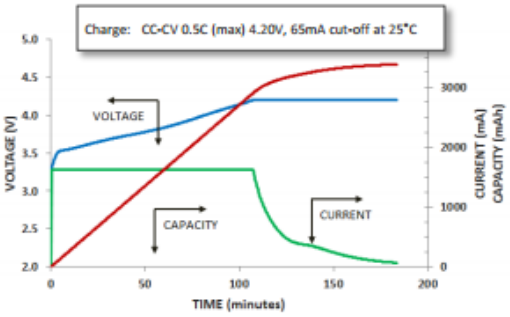

Cycle Life Characteristics

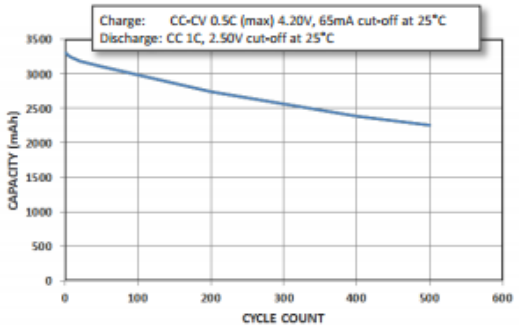

Discharge Characteristics (by temperature)

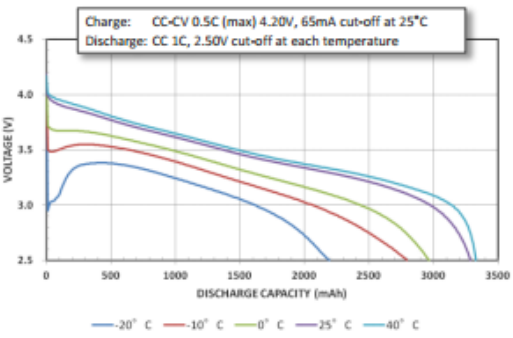

Discharge Characteristics (by rate of discharge)

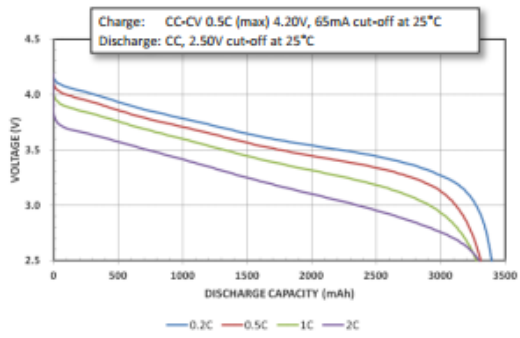

The data in this document is for descriptive purposes only and is not intended to make or imply any guarantee or warranty.

3. SCALED CURRENT VALUES

Selected commute speed and time from [1] (top panel) and corresponding scaled down current for the cycling experiment based on a 30 BSF (bottom panel). The currents displayed in the bottom panel corresponds to the current the batteries would need to deliver to match the speed of the top panel in an hypothetical EV 30 times smaller than the one used in the field.